Flow Turbulence Combust (2012) 89:563–587
DOI 10.1007/s10494-012-9408-x

Efficiency of Scale-Similarity Model for Study of Forced Compressible Magnetohydrodynamic Turbulence

Alexander Chernyshov · Kirill Karelsky · Arakel Petrosyan

Received: 18 October 2011 / Accepted: 19 July 2012 / Published online: 11 August 2012

Abstract Efficiency of scale-similarity model for study of forced compressible magnetohydrodynamic turbulence is studied. The scale-similarity model has several important advantages in contrast to the eddy-viscosity subgrid closures: good reproduction of the correlation between actual and model turbulent stress tensor even when the flow is highly anisotropic, and absence of special model constants. These advantages may be very essential for study of forced magnetohydrodynamic turbulence. Numerical computations under various similarity parameters are carried out and the obtained results are analyzed by means of comparison with results of direct numerical simulation and Smagorinsky closure for magnetohydrodynamics. Linear forcing algorithm is applied to keep the characteristics of turbulence stationary in time. Influence of discrete filter shapes on the scale-similarity model is studied as well. It is shown that the scale-similarity model provides good accuracy and the results agree well with the direct numerical simulation results. The present results show that the scale-similarity model might be a useful subgrid closure for study of scale-invariance properties of forced compressible magnetohydrodynamic turbulence in the inertial range and in contrast to decaying case the scale-similarity model can serve as a stand alone subgrid model.

Keywords Large Eddy simulation · Forced turbulence · MHD · Subgrid-scale modeling · Compressible flow

1 Introduction

Large-Eddy simulation (LES) method is conquering more and more new areas of application, for example, magnetohydrodynamics (MHD) [1, 2, 11–17, 21, 23–25, 34,

A. Chernyshov (✉) · K. Karelsky · A. Petrosyan
Theoretical section, Space Research Institute of Russian Academy of Sciences,
Profsoyuznaya 84/32, Moscow 117997, Russia
e-mail: achernyshov@iki.rssi.ru

43]. A study of various problems of MHD both in applied industry problem and in a space, astrophysical, helio- or geophysical flows requires large-scale modeling of the real physical conditions. Development of efficient numerical techniques and up-to-date computer systems allows to carry out realistic MHD simulation of the turbulent flows. These simulations are extremely important for understanding the complex physics especially when object is beyond the reach of direct experimental study. Note that the MHD problems differ from those of the neutral fluid hydrodynamics. The MHD equations contain two fields, which introduces considerably more freedom into the dynamics, for instance the presence of both direct and inverse spectral cascades [4]. Also, there are self-organization processes in MHD turbulence that have no hydrodynamic counterpart, namely, conservation of cross-helicity [45] leads to highly correlated, or aligned, states, while conservation of magnetic helicity [5] gives rise to the formation of force-free magnetic configurations.

In general, new applications of LES put old questions concerning the use of subgrid-scale (SGS) models. There is no guarantee that the results obtained for hydrodynamics neutral fluid can be directly extended to the case of MHD in consequence of the above-mentioned distinctions. Determination of the optimal SGS parameterizations is a separate non-trivial task especially for forced MHD turbulence. Moreover, LES is not as well established in MHD turbulence as it is in hydrodynamics because the physics is more complex. Experimental verification of the validity of a subgrid-scale model and the calibration of model parameters are very difficult, since MHD turbulence is mainly observed in astrophysical systems and not in controllable laboratory experiments [4]. It is therefore desirable to have subgrid closure without model constants since it is impossible to obtain model constants from in situ measurements in many application MHD turbulence in problems of aerospace industry and astrophysics. It is worth noting that the problem become more complicated when the compressible fluid is considered. The effect of compressibility on the structure of turbulence is an important and difficult topic in turbulence modeling. In order to solve such problems, LES approach is a useful and perspective method.

Aim of the present study is further development of LES approach for MHD turbulence. The LES method is based upon the idea that some scales of the turbulent motion are discarded to obtain a desired reduction in the range of scales required for numerical simulation. In other words, small scales of the turbulent flow are supposed to be more universal according to the local isotropy hypothesis which was suggested by Kolmogorov [26] and less determined by boundary conditions than the large ones in different turbulent problems. LES consists of solving the set of governing equations for fluid mechanics on a discrete grid as all simulation techniques, that is, using a finite number of degrees of freedom [19]. The number of degrees of freedom is smaller than in the direct numerical simulation (DNS) approach. Thus, LES implies much smaller computational costs than DNS. According to LES theory, the large-scale part of the flow is computed directly and only small-scale structures of turbulence are modeled. The small-scale motion is eliminated from the initial system of equations by filtering procedures and their effect is taken into account by special closures referred to as the subgrid-scale models. The SGS models are classifies as functional and structural models [38]. Functional models approximate the action of subgrid scales on the resolved scale (parameterizations of eddy-viscosity type belong to the group of functional models). This action is usually describe by energy transfer. Structural models approximate the SGS stress itself by using the resolved variables

(scale-similarity closures). For the testing of subgrid-models, a priori and a posteriori tests are used.

Different SGS parameterizations have been proposed mostly for incompressible turbulence of neutral fluids. Majority of the works, in which the tests and comparisons SGS closures with DNS results were carried out, have been made for decaying turbulence. Usually, the best results demonstrate eddy-viscosity models or/and mixed SGS models in a posteriori tests. But scale-similarity model shows a lack of energy dissipation. It is well known that the most important features of a SGS closure is to provide adequate dissipation. The overall conclusion is that it is necessary to use the scale-similarity model only together with eddy viscosity model (for example, with the Smagorinsky closure, that provided a basis idea for mixed SGS model). However, in a priori tests, the scale-similarity model reproduces the correlation between this model and actual turbulent stress tensor very well even when the flow is highly anisotropic [18]. This indicate that the similarity model predicts important structures of the turbulent stress at the right locations. One of the main advantages of the scale-similarity model is that it does not require a determination of special model constants in contrast to the eddy-viscosity parameterizations. Although, if the second filter which is wider than the basic model filter is used, one can get a model with a scaling constant that is determined dynamically or chosen from numerical experiments [32, 33]. However, such closure does not offer unambiguous advantages, and a choice of model coefficient values that are different from zero leads to the Galilean non-invariance [41]. Also, although scale-similarity model of integrated dissipative, it can provide local generation of energy. However, when implemented in simulations, the similarity model alone does not dissipate sufficiently energy and typically leads to inaccurate results in decaying cases of magnetohydrodynamic and hydrodynamic turbulence [13, 44].

In the present work, the scale-similarity model for the case of forced compressible MHD turbulence is investigated. For the study of scale-invariance properties of forced compressible MHD turbulence in the inertial range with the use of LES technique, scale-similarity model can produce more accurate results in comparison with models of eddy-viscosity type. In a forced turbulence, driving forces are introduced to inject energy into a turbulent flow, otherwise this flow becomes laminar due to phenomena of viscosity and diffusion. Consequently, in this case SGS modeling have to provide correct statistically stationary regime of the turbulence and not only to assure adequate energy dissipation. Therefore, in the present paper LES with scale-similarity model is studied for compressible magnetohydrodynamic turbulence. Computations are made for compressible MHD flows with magnetic Reynolds numbers smaller than those displaying dynamo actions [10]. Comparison of results of scale-similarity model with eddy-viscosity SGS closure (in this work, extended Smagorinsky model for MHD case is applied since this model is still the most popular and widely used for both MHD and hydrodynamic tasks) and with the DNS results of three-dimensional forced compressible MHD turbulence is carried out under a variety of similarity parameters. The scale-similarity model has several critical advantages mentioned above that may be important to study the scale-invariant properties of the MHD turbulent motion. One might expect that results of modeling of compressible MHD turbulence with driving forces using the scale-similarity model will be sufficiently accurate and, thus, in contrast to decaying case this closure can serve as a stand alone SGS model. It should be noted that

Elsasser variables are often used in magnetic hydrodynamics to write system of MHD equations in a more symmetric form and therefore it is especially important to have a good correlation between SGS and actual turbulent tensors in this case. For instance, strong correlation between all three components of the fluctuating velocity and the magnetic field are observed in the solar wind and it is shown that spectral index for the total energy spectrum may depend on the correlation level [22]. It is also possible that a good correlation is important in problems where there are inhomogeneities of the turbulent flow of charged fluid.

In our work, we use "linear forcing" scheme [17, 31, 37, 42]. Linear forcing algorithm is applied to keep the characteristics of turbulence stationary in time. Linear forcing is very fast because there is no need to transform from a spectral to physical space. The idea behind is that writing the transport equation for fluctuation velocity, the production term is proportional to the fluctuation velocity. The coefficient is the indicator of the balance between the production and dissipation. Since compressible MHD turbulence is considered in the present paper, the system of MHD equations includes the magnetic induction equation, and in this case the driving force is proportional to the magnetic field in the induction equation [17].

The structure of the paper is the following. The next Section 2 describes briefly LES method and "linear forcing" theory to drive stationary compressible MHD turbulence in physical space. We generalize linear forcing method and use these driving forces for modeling of three-dimensional forced compressible MHD turbulence by DNS and LES methods. The SGS models under consideration, numerical setups, influence of discrete filter shapes on scale-similarity model, test configurations and analysis of obtained results are specified in Section 3. Three numerical cases are performed under various similarity numbers, namely, magnetic and hydrodynamic Reynolds numbers, magnetic and sonic Mach numbers (all runs are subsonic with Mach numbers between 0.23 and 0.52). Finally, conclusions are given in the last Section 4.

2 Large Eddy Simulation of Forced Compressible MHD Turbulence

In this section, the general features of LES method for modeling of compressible MHD turbulence with external driving forces are presented. We briefly describe "linear forcing" theory for the case of compressible magnetohydrodynamic turbulence. The expressions for driving forces in the momentum conservation equation and in the magnetic induction equation for modeling of forced MHD turbulence in physical space for LES approach are shown.

We write the filtered MHD equations for compressible flow [13, 17] in dimensionless form using the standard procedure [4]:

$$\frac{\partial \bar{\rho}}{\partial t} + \frac{\partial \bar{\rho}\tilde{u}_j}{\partial x_j} = 0; \tag{1}$$

$$\frac{\partial \bar{\rho}\tilde{u}_i}{\partial t} + \frac{\partial}{\partial x_j}\left(\bar{\rho}\tilde{u}_i\tilde{u}_j + \frac{\bar{\rho}^\gamma}{\gamma M_s^2}\delta_{ij} - \frac{1}{Re}\tilde{\sigma_{ij}} + \frac{\bar{B}^2}{2M_a^2}\delta_{ij} - \frac{1}{M_a^2}\bar{B}_j\bar{B}_i\right) = -\frac{\partial \tau_{ji}^u}{\partial x_j} + \tilde{F}_i^u; \tag{2}$$

$$\frac{\partial \bar{B}_i}{\partial t} + \frac{\partial}{\partial x_j}\left(\tilde{u}_j \bar{B}_i - \tilde{u}_i \bar{B}_j\right) - \frac{1}{Re_m}\frac{\partial^2 \bar{B}_i}{\partial x_j^2} = -\frac{\partial \tau_{ji}^b}{\partial x_j} + \bar{F}_i^b; \tag{3}$$

$$\frac{\partial \bar{B}_j}{\partial x_j} = 0, \tag{4}$$

where ρ is the density; u_j is the velocity in the direction x_j; B_j is the magnetic field in the direction x_j; $\sigma_{ij} = 2\mu S_{ij} - \frac{2}{3}\mu S_{kk}\delta_{ij}$ is the viscous stress tensor; $S_{ij} = 1/2\left(\partial u_i/\partial x_j + \partial u_j/\partial x_i\right)$ is the strain rate tensor; μ is the coefficient of molecular viscosity; η is the coefficient of magnetic diffusivity; δ_{ij} is the the Kronecker delta; F_i^u and F_i^b are the driving forces; Re is the Reynolds number; Re is the magnetic Reynolds number; M_s is the Mach number and M_a is the magnetic Mach number.

In LES method every physical parameter is expanded into large-scale and small-scale components. After that, the large-scale effects are computed directly, while the small-scale ones are modeled. To filter the equations of the magnetohydrodynamics, the LES technique uses filter ξ satisfying the normalization property. Filtering procedure is applied to the governing MHD equations. The filtered (or large-scale) part $\bar{\zeta}(x_i)$ is defined by the following way:

$$\bar{\zeta}(x_i) = \int_\Theta \zeta(\acute{x}_i)\xi\left(x_i, \acute{x}_i; \bar{\triangle}\right) d\acute{x}_i, \tag{5}$$

where ξ is the filter function, ζ is a flow parameter, Θ is the flow domain, $\bar{\triangle}$ is the filter-width and $x_j = (x, y, z)$ are axes of Cartesian coordinate system. Filter ξ satisfies the normalization property: $\int_\Theta \xi(x_i, \acute{x}_i; \bar{\triangle}) d\acute{x}_j = 1$ for any $x \in \Theta$.

To simplify equations describing turbulent MHD flow with variable density it is convenient to use Favre filtering (known as mass-weighted filtering) so as to avoid appearance of additional SGS-terms. Therefore, Favre filtering will be used further. Mass-weighted filtering is used for all parameters of charged fluid flow besides the pressure and magnetic fields. Mass-weighted filtering is determined as follows

$$\tilde{\zeta} = \frac{\overline{\rho\zeta}}{\bar{\rho}}. \tag{6}$$

Filtration is designated by two symbols in Eq. 6, namely, the overline designates ordinary filtering, while the tilde specifies mass-weighted filtering. Therefore, the Favre filtered values can be presented in the form of a sum, for instance, for the velocity: $u = \tilde{u} + u''$. Here the double prime designates small-scale part of the Favre filtered value.

To close the system of Eqs. 1–4 it is assumed that the relation between density and pressure is polytropic [10] and has the following form: $p = \rho^\gamma$, where γ is a polytropic index.

The first terms in right-hand sides in the Eqs. 2 and 3 contain turbulent tensors τ_{ij}^u and τ_{ij}^b that designate influence of subgrid-scale terms on the filtered part: $\tau_{ij}^u = \bar{\rho}\left(\widetilde{u_i u_j} - \tilde{u}_i\tilde{u}_j\right) - \frac{1}{M_a^2}\left(\overline{B_i B_j} - \bar{B}_i\bar{B}_j\right)$ and $\tau_{ij}^b = \left(\overline{u_i B_j} - \tilde{u}_i\bar{B}_j\right) - \left(\overline{B_i u_j} - \bar{B}_i\tilde{u}_j\right)$. The goal of SGS modeling is to account for the SGS stresses using resolved flow fluid variables. The subgrid scales appear in the system of equations as a term called SGS stress which can not be written in terms of filtered variables. Some SGS models try

to model these SGS stresses, and some models include the interaction between large and small scales.

There are external driving forces F_i^u and F_i^b on the right-hand sides of Eqs. 2 and 3 respectively. Driving forces F_i^u and F_i^b which sustain turbulence are necessary to study statistically stationary flow and provide a stationary picture of the energy cascade and more statistical sampling. If energy is not injected into a turbulent flow, after some time this flow becomes laminar because of viscosity and diffusion. To sustain a three-dimensional turbulence, a driving force is employed to inject energy in the turbulent system to replace the energy which is dissipated on small spatial scales.

Recently, so-called "linear forcing" [31] was suggested and used for modeling of hydrodynamic turbulence of neutral fluid [37, 42] and compressible MHD turbulence [17] with driving force in physical space. The idea essentially consists of adding a force proportional to the fluctuating velocity. Linear forcing resembles a turbulence when forced with a mean velocity gradient, that is, a shear. This force appears as a term in the equation for fluctuating velocity that corresponds to a production term in the equation of turbulent kinetic energy. In compressible MHD turbulence, system of MHD equations includes also the magnetic induction equation and in this case the driving force is proportional to the magnetic field in the magnetic induction equation [17]. Thus, linear external force can be interpreted as the production of magnetic energy due to the interaction between the magnetic field and the mean fluid shear. Below we describe briefly determination of the expressions for external forces.

The equation for the fluctuating part of the velocity in a compressible MHD turbulent flow are written in dimensional form as

$$\rho\left[\frac{\partial \acute{u}_i}{\partial t}+U_j\frac{\partial \acute{u}_i}{\partial x_j}\right]=-\frac{\partial \acute{p}}{\partial x_j}+\frac{\partial \acute{\sigma}_{ij}}{\partial x_j}-\rho\acute{u}_j\frac{\partial U_i}{\partial x_j}-\left[\rho\acute{u}_j\frac{\partial \acute{u}_i}{\partial x_j}-\rho\left\langle\acute{u}_j\frac{\partial \acute{u}_i}{\partial x_j}\right\rangle\right]$$
$$-\frac{\partial}{\partial x_j}\frac{\acute{B}^2}{8\pi}+\frac{1}{4\pi}\left[ß_j\frac{\partial \acute{B}_i}{\partial x_j}+\acute{B}_j\frac{\partial ß_i}{\partial x_j}\right]+\frac{1}{4\pi}\left[\acute{B}_j\frac{\partial \acute{B}_i}{\partial x_j}-\left\langle\acute{B}_j\frac{\partial \acute{B}_i}{\partial x_j}\right\rangle\right] \quad (7)$$

Here the following decomposition, referred to as the Reynolds decomposition, is used: $u_i = U_i + \acute{u}_i$, $B_i = ß_i + \acute{B}_i$, $p = P + \acute{p}$, $\sigma_{ij} = \Sigma_{ij} + \acute{\sigma}_{ij}$, where U_i, $ß_i$, Σ_{ij}, P represent the mean motion, and $\acute{u}_i$, $\acute{B}_i$, $\acute{\sigma}$, $\acute{p}$ are the fluctuating values.

The third term $\rho\acute{u}_j(\partial U_i/\partial x_j)$ on the right-hand side in the Eq. 7 corresponds to the production term in the turbulent kinetic energy equation. The equation for the turbulent kinetic energy follows by taking the scalar product of the velocity with the unaveraged momentum equation, statistically averaging this equation, and then subtracting from it the scalar product of the mean velocity with the statistically averaged momentum conservation equation. In symbolic terms, derivation of the turbulent kinetic energy equation can be written as $\langle v \cdot \textit{momentum eq.}\rangle - U \cdot \langle \textit{momentum eq.}\rangle$ (where *momentum eq.* implies Navier-Stocks equation with Lorentz force), which yields:

$$\frac{\partial}{\partial t}\left\langle\frac{1}{2}\rho\acute{u}^2\right\rangle+\frac{\partial}{\partial x_j}\left(\left\langle\frac{1}{2}\rho\acute{u}^2\right\rangle U_j+\left\langle\frac{1}{2}\rho\acute{u}^2\acute{u}_j\right\rangle-\langle\beta_{ij}\acute{u}_i\rangle\right)$$
$$=-\left\langle\acute{u}_i\frac{\partial \acute{p}}{\partial x_i}\right\rangle+\left\langle\acute{u}_i\frac{\partial \acute{\sigma}_{ij}}{\partial x_j}\right\rangle-\langle\rho\acute{u}_i\acute{u}_j\rangle\frac{\partial U_i}{\partial x_j}-\left\langle\beta_{ij}\frac{\partial \acute{u}_i}{\partial x_j}\right\rangle \quad (8)$$

where β_{ij} is the turbulent magnetic stress expressed in the form:

$$\beta_{ij} = \frac{\acute{B}_i \acute{B}_j}{4\pi} - \frac{\acute{B}^2}{8\pi}\delta_{ij} \tag{9}$$

In the Eq. 8 the term $\langle \rho \acute{u}_i \acute{u}_j \rangle \frac{\partial U_i}{\partial x_j}$ is the production of turbulent energy per unit volume per unit time resulting from the interaction between the Reynolds stress and the mean shear. In Eq. 7, it can be interpreted as the term with a driving force which is directly proportional to v. Thus, this suggests that for isotropic homogeneous turbulence it might be appropriate to force a stationary flow with a driving term proportional to the velocity:

$$F_i^u = \Theta \rho u_i \tag{10}$$

where Θ is the coefficient which is determined from a balance of kinetic energy for a statistically stationary state. The forcing function $F_i^u = \Theta \rho u_i$ in the physical space is equivalent to force all the Fourier modes in the spectral space. This is in fact the only difference from the standard spectral forcing when energy is added in to system only in the range of small wave numbers (wavenumber shell), that is, in integrated (large) scale of turbulence. It should be pointed out that the coefficient Θ can be constant during the simulation that is equivalent to imposing a prescribed turnover time scale. However, the coefficient Θ can be recalculated during a simulation using the current velocity [37].

The determination of the driving force F_i^b in the magnetic induction equation is similar:

$$F_i^b = \Psi B_i \tag{11}$$

Here Ψ is the coefficient. The coefficient Ψ is determined from the balance of magnetic energy for the statistically stationary state as well. More detailed derivation and information about linear forcing method for compressible MHD turbulence can be found in our article [17].

In this work, the forces F_i^u and F_i^b are defined by means of the theory of linear forcing in Eqs. 10 and 11, and have the following dimensionless form:

$$\tilde{F}_i^u = \frac{1}{3\langle \bar{\rho} \rangle \tilde{u}_{rms}^2} \left[\tilde{\varepsilon} + \aleph + \frac{\langle \tilde{u}_j \frac{\partial}{\partial x_j} \bar{\rho}^\gamma \delta_{ij} \rangle}{\gamma M_s^2} + \frac{\langle \tilde{u}_j \frac{\partial}{\partial x_j} \bar{B}^2 \delta_{ij} \rangle}{2 M_a^2} \right] \bar{\rho} \tilde{u}_i \tag{12}$$

$$\bar{F}_i^b = \frac{\chi + \hbar}{3 \bar{B}_{rms}^2} \bar{B}_i \tag{13}$$

Here $\tilde{\varepsilon} = -\langle \frac{\tilde{u}_j}{Re} \frac{\partial \tilde{\sigma}}{\partial x_j} \rangle$ is the mean dissipation rate of turbulent energy into heat. The term $\aleph = \langle \tilde{u}_j \frac{\partial \tau_{ij}^u}{\partial x_j} \rangle$ represents the SGS dissipation which, in fact, is rate at which energy is locally transferred from energetic resolved eddies to unresolved residual motions. Moreover, it is taken into account in Eq. 12 that $1/(\langle \rho u^2 \rangle) = 1/(3\langle \rho \rangle u_{rms}^2)$, because $u_{rms}^2 = (\langle \rho u^2 \rangle)/(3\langle \rho \rangle)$ is a mass-averaged root-mean-square velocity. Note that in compressible homogenious turbulence the term $\langle u_j (\partial p / \partial x_j) \rangle = -\langle p (\partial u_j / \partial x_j) \rangle$. The expression $\chi = \langle \bar{B}_i \frac{\partial^2 \bar{B}_i}{\partial x_j^2} \rangle$ is resistive dissipation of the turbulent magnetic energy

in MHD turbulence. The term $\hbar = \langle \tilde{B}_i \frac{\partial \tau_{ij}^b}{\partial x_j} \rangle$ represents the magnetic SGS energy dissipation. The term $B_{rms}^2 = \langle B^2 \rangle / 3$ is the root-mean-square magnetic field.

Note that additional term associated with subgrid-scale tensor arises in an energy balance when defining a coefficient in the expression for the driving force when LES technique is used. If eddy-viscosity SGS model (for example, Smagorinsky closure) and dynamic procedure for definition of model constants are applied, these additional terms $\aleph$ and $\hbar$ can be omitted because values of these model constants are self-consistently computed during run time using the dynamic procedure in LES. In the dynamic procedure, model constants are chosen to minimize (applying least-squares method) the dependence of turbulent statistics on the filter-width $\bar{\triangle}$ [36]. Consequently, the dynamic constant should adjust to an appropriate value. However, in the present work, we use not only the Smagorinsky model but the scale-similarity parametrization in which there is not model constant. Therefore, the terms $\aleph$ and $\hbar$ do not omit in the expressions 12 and 13, that is, $\aleph$ and $\hbar$ compute explicitly at definition of coefficients of the driving forces in LES method. The linear representation of the driving force may also be of use in the DNS approach. The difference is only in the absence of the terms $\aleph$ and $\hbar$ are associated with the use of SGS closures.

3 SGS Modeling and Computational Results

In the present section, the subgrid-scale modeling in LES is discussed and the numerical methods used for computations of forced magnetohydrodynamic turbulence by means of DNS and LES approaches are described. The obtained numerical LES results are analyzed on a basis of comparison with the results of numerical experiments performed by direct numerical simulation.

Any turbulent SGS tensor can be decomposed into three parts [27], for instance for τ_{ij}^u:

$$\begin{aligned}
\tau_{ij}^u &= \bar{\rho}\left(\widetilde{u_i u_j} - \tilde{u}_i \tilde{u}_j\right) - \frac{1}{M_a^2}\left(\overline{B_i B_j} - \bar{B}_i \bar{B}_j\right) \\
&= \underbrace{\bar{\rho}\left(\widetilde{\tilde{u}_i \tilde{u}_j} - \tilde{u}_i \tilde{u}_j\right) - \frac{1}{M_a^2}\left(\overline{\bar{B}_i \bar{B}_j} - \bar{B}_i \bar{B}_j\right)}_{\text{Leonard term}} \\
&\quad + \underbrace{\bar{\rho}\left(\widetilde{\tilde{u}_i u_j''} + \widetilde{\tilde{u}_j u_i''}\right) - \frac{1}{M_a^2}\left(\overline{\bar{B}_i B_j'} + \overline{\bar{B}_j B_i'}\right)}_{\text{Cross term}} + \underbrace{\bar{\rho}\left(\widetilde{u_i'' u_j''}\right) - \frac{1}{M_a^2}\left(\overline{B_i' B_j'}\right)}_{\text{Reynolds–Maxwell term}} \\
&= L_{ij} + C_{ij} + R_{ij}
\end{aligned} \tag{14}$$

In the expression 14, the Leonard stress L_{ij} describes the interaction between the resolved scales [27]. The cross term C_{ij} represents the interaction between the resolved and SGS motion. Finally, the third term, R_{ij}, the Reynolds–Maxwell stress tensor describes the interaction between the subgrid scales and is responsible for the energy dissipation. In fact, the Reynolds–Maxwell stress is familiar from RANS and represents the advection of subgrid scales by turbulent fluctuations. In general,

there are two main approaches to turbulent stress modeling in LES. The first one is called scale similarity. It concentrates the attention at the Leonard term L_{ij}, that is, SGS tensors are proportion the Leonard stress tensor $\tau_{ij} \propto L_{ij} \propto L_{ij} + C_{ij} + R_{ij}$. The second approach is called eddy viscosity. It focuses on the Reynolds (or Reynolds–Maxwell) term R_{ij} and assumes that $\tau_{ij} \propto R_{ij}$.

The first scale-similarity model was proposed by Bardina et al. [3] and its other version was investigated by Liu et al. [29] for LES of incompressible flows. Further study was performed by Meneveau and Katz [32]. Bardina et al. [3] apply the assumption that the largest unresolved scales are similar to the smallest resolved scales of turbulent flow and use the filter twice to separate the smallest and largest resolved scales. The largest unresolved scales are approximated by smallest resolved scales, for example, for the velocity: $u_i'' \approx \tilde{u}_i'' \approx \tilde{\tilde{u}}_i - \tilde{u}_i$. This assumption leads to the following possibility as a subgrid-scale closure for compressible MHD case [13]:

$$\tau_{ij}^u = \bar{\rho}\left(\widetilde{\tilde{u}_i\tilde{u}_j} - \tilde{\tilde{u}}_i\tilde{\tilde{u}}_j\right) - \frac{1}{M_a^2}\left(\overline{\bar{B}_i\bar{B}_j} - \bar{\bar{B}}_i\bar{\bar{B}}_j\right) \tag{15}$$

$$\tau_{ij}^b = \left(\overline{\tilde{u}_i\bar{B}_j} - \tilde{\tilde{u}}_i\bar{\bar{B}}_j\right) - \left(\overline{\bar{B}_i\tilde{u}_j} - \bar{\bar{B}}_i\tilde{\tilde{u}}_j\right) \tag{16}$$

It is apparent that, the scale-similarity model 15 and 16 can be calculated in a LES by means of the filtered variables in contrast to eddy-viscosity parameterizations. Model constants in Eqs. 15 and 16 are not introduced as this would destroy the Galilean invariance of the expression [41].

We compare the results of scale-similarity model not only with DNS-results but with numerical results of Smagorinsky closure. Smagorinsky model was one of the first SGS parameterizations and is the most popular and widely used in various computations. The Smagorinsky SGS closure is based on the eddy-viscosity concept. The eddy-viscosity concept assumes that the energy transfer mechanism from the large scales to the small scales is similar to the molecular mechanism represented by the diffusion term. We use extended Smagorinsky model for compressible MHD case for SGS parametrization [11, 13]. The Smagorinsky model showed accurate results in a wide range of similarity numbers in decaying compressible MHD turbulence [13]:

$$\tau_{ij}^u - \frac{1}{3}\tau_{kk}^u\delta_{ij} = -2C_1\bar{\rho}\bar{\Delta}^2|\tilde{S}^u|\left(\tilde{S}_{ij} - \frac{1}{3}\tilde{S}_{kk}\delta_{ij}\right), \tag{17}$$

$$\tau_{ij}^b = -2D_1\bar{\Delta}^2|\bar{j}|\bar{J}_{ij}, \tag{18}$$

$$\tau_{kk}^u = 2Y_1\bar{\rho}\bar{\Delta}^2|\tilde{S}^u|^2 \tag{19}$$

Coefficients C_1, Y_1 and D_1 in the Eqs. 17–19 are model constants calculated using dynamical procedure [11, 20, 34] in our work.

We perform three-dimensional numerical simulation of forced compressible MHD turbulence in physical space and the numerical code of the fourth order accuracy for MHD equations in the conservative form based on non-spectral finite-difference schemes is used in our work. The third order low-storage Runge–Kutta

method [8] is applied for time integration. The skew-symmetric form of nonlinear terms for modeling of turbulent flow is applied to reduce discretization errors. The skew-symmetric form is a form obtained by averaging divergent and convective forms of the nonlinear terms:

$$\Psi_i^d = \frac{(\partial \rho u_i u_j)}{\partial x_j}$$
$$\Psi_i^a = \rho u_j \frac{\partial u_i}{\partial x_j} + u_i \frac{(\partial \rho u_j)}{\partial x_j}$$
$$\Psi_i^s = \frac{1}{2}\left(\Psi_i^d + \Psi_i^a\right) \tag{20}$$

In spite of analytical equivalence of all three forms, their numerical realizations give different results and it was shown that skew-symmetric form improves computational accuracy for turbulent modeling. Periodic boundary conditions for all the three dimensions are applied. The simulation domain is a cube $\pi \times \pi \times \pi$. The mesh with 64^3 grid cells is used for LES and 256^3 for DNS. The explicit LES method is used in this work. The model constants in the Smagorinsky closures are determined by means of dynamic procedure [11, 34]. The initial isotropic turbulent spectrum close to k^{-2} with random amplitudes and phases in all three directions was chosen for kinetic and magnetic energies in Fourier space. The choice of such spectrum as initial conditions is due to velocity perturbations with an initial power spectrum in Fourier space similar to that of developed turbulence [30]. This k^{-2} spectrum corresponds to spectrum of Burgers turbulence. Initial conditions for the velocity and the magnetic field have been obtained in the physical space using inverse Fourier transform. The results obtained with Large Eddy simulation are compared with DNS computations and performance of Large Eddy simulation is examined by difference between LES- and filtered DNS-results. The initial conditions for LES are obtained by filtering the initial conditions of DNS.

3.1 Sensitivity of scale-similarity model on the filter shape for MHD case

There is strong influence of the nature of the LES filter on the interactions between resolved and subgrid-scales. First, we examine the question of the effect of different filter shapes on scale-similarity model for compressible MHD turbulence using a finite-difference schemes for modeling. Several papers were devoted to this problem for a neutral fluid hydrodynamics, both theoretical and numerical studies have been carried out (for example, [28, 35, 39, 40]). To our knowledge, until now the influence of discrete filters on the scale-similarity model for the case of compressible forced MHD turbulence is not performed, so we will briefly examine this effect before the comparison the results of scale-similarity closure with results of DNS and Smagorinsky parametrization.

It should be remarked that the definition 5 is too general. The real flows can be investigated with the help of some simpler appropriate filter. Since the finite-difference schemes for simulation of MHD turbulence are used in this paper, we consider the Gaussian filter and the top-hat filter. They are commonly applied

when using non-spectral modeling techniques in physical space. The top-hat filter is defined as:

$$\xi(x,\acute{x}) = \begin{cases} \frac{1}{\bar{\Delta}}, \text{ if } \mid x-\acute{x} \mid \leq \frac{\bar{\Delta}}{2} \\ 0, \text{otherwise} \end{cases} \tag{21}$$

The Gaussian filter is:

$$\xi(x,\acute{x}) = \left(\frac{6}{\pi\bar{\Delta}^2}\right)^{1/2} exp\left(-\frac{6 \mid x-\acute{x} \mid^2}{\bar{\Delta}^2}\right)^{1/2} \tag{22}$$

Filter approach was analyzed by Sagaut and Grohens [40]. They were looking for an optimal shape of the filters which is consistent with the numerical scheme in use. They found by means of the Taylor series decomposition that the top-hat and Gaussian filters coincide exactly for second order accuracy numerical schemes (using 3 points):

$$\bar{\zeta_i} = \frac{1}{24} * \epsilon^2 * \zeta_{i-1} + \frac{1}{12} * \left(12-\epsilon^2\right) * \zeta_i + \frac{1}{24} * \epsilon^2 * \zeta_{i+1} \tag{23}$$

Fourth order accuracy numerical schemes (using 5 point) consistent with different forms of these filters. Operator equivalent to the fourth-order Gaussian filter and top-hat filter respectively are:

$$\bar{\zeta_i} = \frac{\epsilon^4-4\epsilon^2}{1152}(\zeta_{i-2}+\zeta_{i+2}) + \frac{16\epsilon^2-\epsilon^4}{288}(\zeta_{i-1}+\zeta_{i+1}) + \frac{\epsilon^4-20\epsilon^2+192}{192}\zeta_i, \tag{24}$$

$$\bar{\zeta_i} = \frac{3\epsilon^4-20\epsilon^2}{5760}(\zeta_{i-2}+\zeta_{i+2}) + \frac{80\epsilon^2-3\epsilon^4}{1440}(\zeta_{i-1}+\zeta_{i+1}) + \frac{3\epsilon^4-100\epsilon^2+960}{690}\zeta_i, \tag{25}$$

Here, ζ_i is the flow parameter in the point i and the parameter ϵ represents the ratio of the mesh size to the cut-off lengthscale of the filter [40]. It is usually assumed that the parameter ϵ is equal to 2 in the works where the fluid flows are modeled by means of LES approach. However, in order to study how this parameter affects the results of the calculation, we consider the cases when the parameter ϵ takes a different value, namely, $\epsilon = 3$.

Initially it should be noted that since the problem considered in this work is three-dimensional three dimensional filter (multidimensional one in the general case) must be constructed. Multidimensional filter can be constructed in two different ways [40]. The first one is a linear combination of one-dimensional filters, i.e. for every direction the flow parameter is filtered independently from the others

$$\xi^n = \frac{1}{n}\sum_{i=1}^{n}\xi^i, \tag{26}$$

where ξ^i is a one-dimensional filter in direction i, n is the number of space dimensions. Linear combination represents simultaneous application of all one-

dimensional filters in every spatial direction. The second approach is a product of one-dimensional filters. In that case the following can be written:

$$\xi^n = \prod_{i=1}^{n} \xi^i. \tag{27}$$

Such technique of determination of multidimensional filter ξ^n represents non-simultaneous application of one-dimensional filters like in the first case but sequential one. The accuracy of constructed the multidimensional filters was tested by Sagaut and Grohens [40]. They showed that sequential product of filters gives more accurate results in comparison with linear combination of one-dimensional filters. Therefore, in this work the sequential product of filters 27 is used for three-dimensional filtration.

Since the dependency of scale-similarity SGS models which rely on the application of a filter to its discrete formulation is investigated, we consider various versions of scale-similarity closure which correspond to various 3- and 5-point approximations of both Gaussian and top-hat filters for $\epsilon = 2$ and $\epsilon = 3$. We use similarity numbers as for the first case (see below initial conditions in the Section 3.2).

Time evolution of b_{rms} and u_{rms} are shown in Figs. 1 and 2 respectively. Here in Figs. 1 and 2, the diamond line is the DNS results, the solid line is 5-point approximation of the Gaussian filter ($\epsilon = 2$), the dashed line is 5-point approximation of the top-hat filter ($\epsilon = 2$), the dash-dot line is 3-point approximation of the Gaussian (or top-hat) filter ($\epsilon = 2$), the circle line is 5-point approximation of the Gaussian filter ($\epsilon = 3$), the triangle line is 5-point approximation of the top-hat filter ($\epsilon = 3$), and the plus line is 3-point approximation of the Gaussian (or top-hat) filter ($\epsilon = 3$).

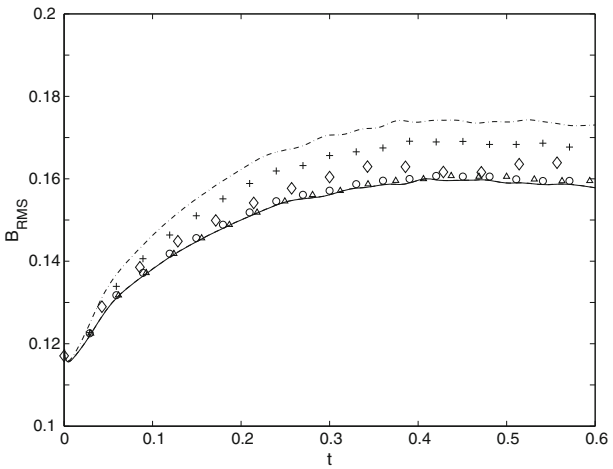

Fig. 1 Time evolution of b_{rms} for various filter shapes. The *diamond line* is the DNS results, the *solid line* is 5-point approximation of the Gaussian filter ($\epsilon = 2$), the *dashed line* is 5-point approximation of the top-hat filter ($\epsilon = 2$), the *dash-dot line* is 3-point approximation of the Gaussian (or top-hat) filter ($\epsilon = 2$), the *circle line* is 5-point approximation of the Gaussian filter ($\epsilon = 3$), the *triangle line* is 5-point approximation of the top-hat filter ($\epsilon = 3$), and the plus line is 3-point approximation of the Gaussian (or top-hat) filter ($\epsilon = 3$)

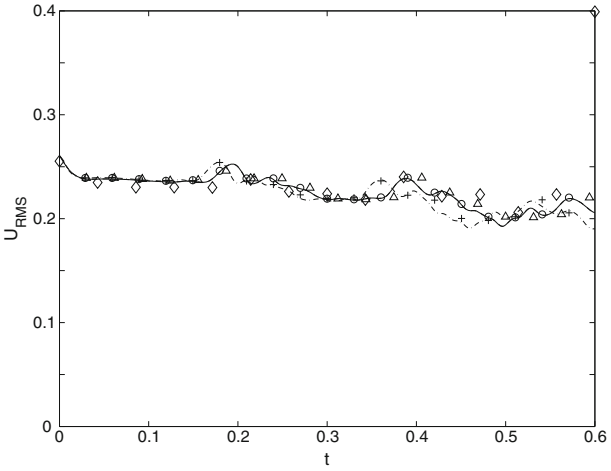

Fig. 2 Time evolution of u_{rms} for various filter shapes. Symbols as in Fig. 1

In these plots, we can see that the use of the 5-point filters lead to a increase of the accuracy. The largest discrepancy with the DNS results is observed for scale-similarity results with the 3-point Gaussian (or top-hat) filters at different values of ϵ. At the same time, the 5-point filters are in good agreement with the "exact" results of DNS. One can notice that 5-point filters lead to similar results for the two values of parameter ϵ whereas a 3-point filter produces more discrepancies for magnetic field. The spectra of total energy E_T^K corresponding to these various cases are shown in Fig. 3. Total energy is the sum of kinetic and magnetic energy $E_T = E_M + E_K$. As expected, the main differences in the results are concentrated on the small scales. In order to observe these differences better, Fig. 4 shows enlargement zone for large values of wave number k. Note that the Gaussian filter is more sensitive to the parameter ϵ than the top-hat one for scale-similarity model in compressible MHD

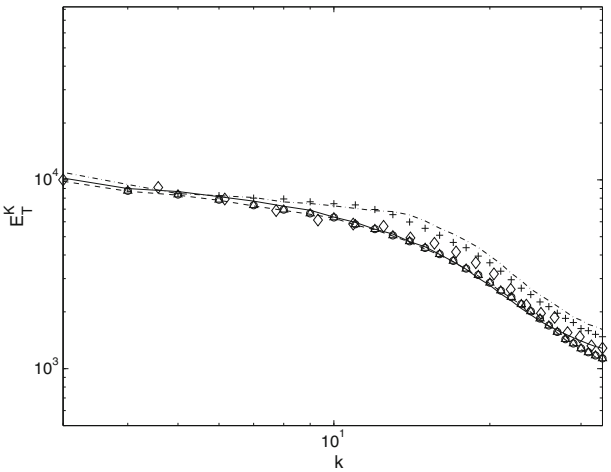

Fig. 3 Total energy spectrum E_T^K for various filter shapes. Symbols as in Fig. 1

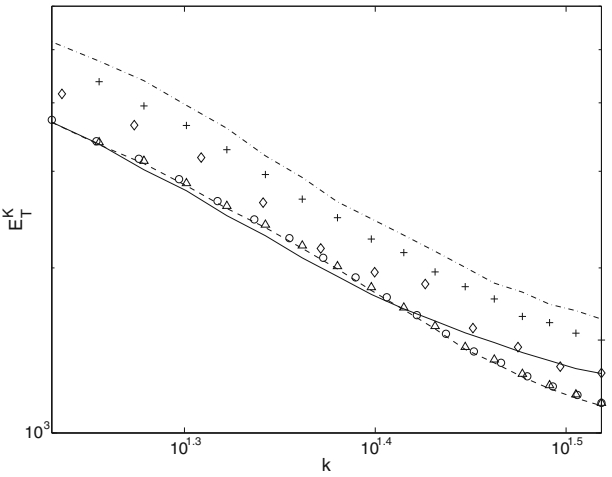

Fig. 4 Total energy spectrum E_T^K in enlargement zone of large values of wave number k for various filter shapes. Symbols as in Fig. 1

turbulence. From our calculations it can be seen that the 3-point filters give the worst results and the 5-point Gaussian filter demonstrates the best results (that is, best approximation to DNS) at $\epsilon = 2$. Notice that the difference between these filters is still within 10 %. Therefore, we use the discrete approximation of the 5-point Gaussian filter hereinafter in this work.

3.2 Validity of scale-similarity model

In this paper we consider several numerical cases varying the similarity parameters. For the first case similarity numbers are: $Re \approx 300$, $Re_M \approx 50$, $M_s \approx 0.35$, $M_a \approx 1.4$, $\gamma = 1.5$. It should be noted that we investigate compressible forced MHD turbulence in the given paper rather than a progress of dynamo-processes in three-dimensional charged fluid flow. The value of the magnetic Reynolds number is chosen from these considerations. The reader could find useful information concerning various methods of modeling of the dynamo-processes and the alpha-effect in the articles [5, 5–7, 7, 9]. Also, note that everywhere in our calculations the forcing coefficient in Eqs. 10 and 11 are recalculated at each time step.

An important criterion for evaluating the quality of LES subgrid models is the correct time evolution of scalar quantities that characterize the global state of the simulated system. Figure 5 shows the time evolution of u_{rms} in physical space. Here in Fig. 5 and hereinafter, the diamond line denotes the DNS values, the solid line is the extended Smagorinsky model for MHD turbulent flow, and the dashed line is the scale-similarity model for MHD. We can see that both SGS models reproduce correctly temporal evolution of root-mean-square velocity. The transient period of u_{rms} is short because of the choice of initial conditions. DNS results have oscillations and LES results are displayed accurately these oscillations. The Smagorinsky model is more dissipative SGS closure than the scale-similarity model as expected. However, both SGS models demonstrate good agreement with DNS results. Time evolution of root-mean-square magnetic field B_{rms} is shown in Fig. 6. Note that the transient period of magnetic field is longer than for velocity.

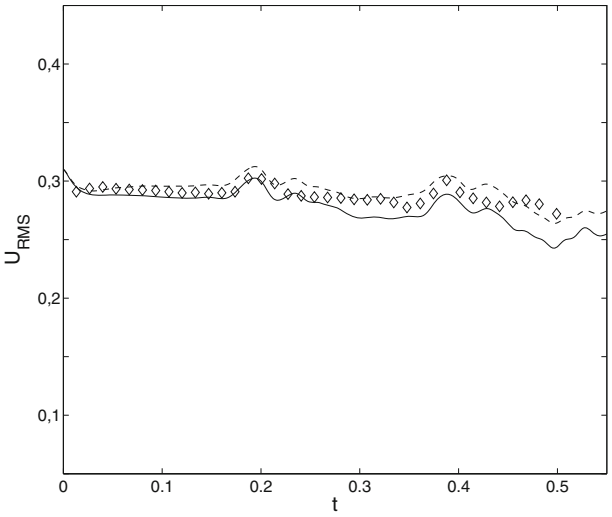

Fig. 5 Time evolution of u_{rms} for the first case. The *diamond line* is the DNS results, the *solid line* is the extended Smagorinsky model for compressible MHD case, and the *dashed line* is the scale-similarity model for compressible MHD turbulence

Both SGS parameterizations achieve a stationary regime correctly and properly, but the scale-similarity model shows more precise coincidence with DNS. Important quantity in magnetohydrodynamics of charged fluid is an evolution of cross-helicity $H^c = \int_V (u \cdot B) dV$. In Fig. 7, time dynamics of the cross-helicity is plotted. Figure 7 demonstrates that initially Smagorinsky model is more accurate but then scale-similarity closure provide better agreement with DNS results. Since compressible MHD turbulence is considered in this paper, it is interesting to study the temporal evolution of the density. Time dynamics of the density is shown in Fig. 8. We compute the density variance as averaged densities at each points of the numerical grid. After initial period, all results fluctuate around the mean value.

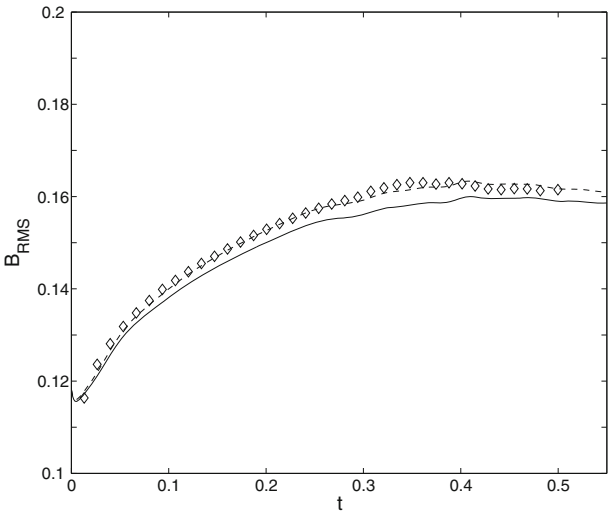

Fig. 6 Time evolution of B_{rms} for the first case. Symbols as in Fig. 5

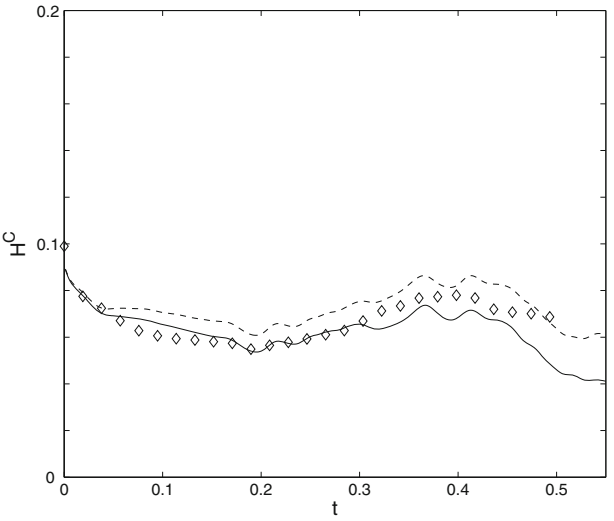

Fig. 7 Cross-helicity H^c as a function of time for the first case. Symbols as in Fig. 5

It is common knowledge that the spectral distribution of the kinetic and the magnetic energies that shows redistribution of energy depending on wave number, i.e., at different scales. The investigation of inertial range properties is one of the main tasks in studies of scale-similarity spectra of MHD turbulence. Inertial range properties are defined as time averages over periods of stationary turbulence conditions. In Fig. 9, total energy spectrum E_T^K is shown. It is worth noting that the famous spectra of Iroshnikov–Kraichnan and Kolmogorov–Obukhov for MHD turbulence were obtained for the total energy. As can be seen from Fig. 9, the scale-similarity model yields more accurate results than Smagorinsky parametrization for MHD case, that is, results of the scale-similarity model produce better conformance

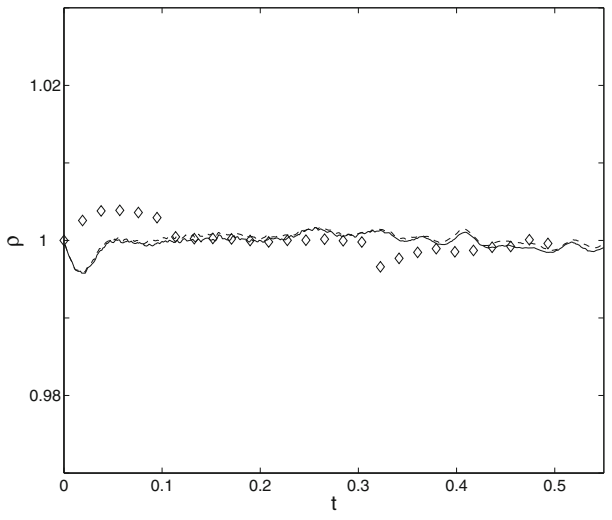

Fig. 8 Time dynamics of the density for the first case. Symbols as in Fig. 5

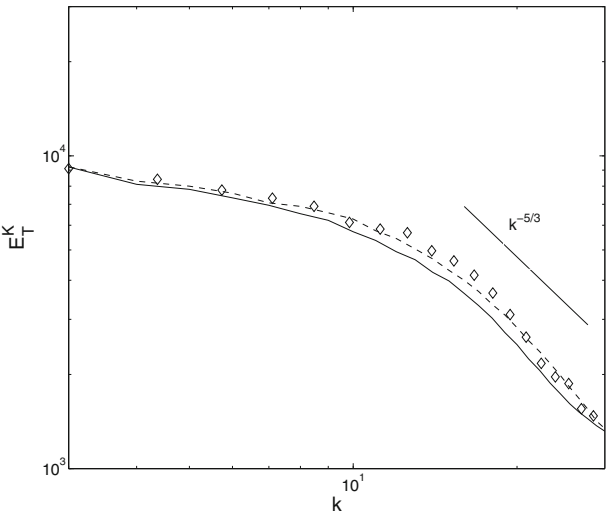

Fig. 9 Total energy spectrum E_T^K for the first case. Symbols as in Fig. 5

with DNS results. As shows in Fig. 9, there is well-defined inertial Kolmogorov-like range of $k^{-5/3}$ for the first case. Thus, subgrid-scale models with linear forcing can correctly reproduce the scale-invariant properties of the MHD turbulent flow. Since MHD turbulence is considered in the work, it is important to know the behavior of the magnetic energy spectrum using different SGS closures. In Fig. 10, magnetic energy spectrum E_M^K is depicted. It is seen that the Smagorinsky and the scale-similarity models demonstrate good agreement with DNS results.

Time evolution of the kinetic energy subgrid scale dissipation is plotted in Fig. 11a. This term, defined here as $\Pi_{sgs}^u = -\tau_{ij}^u \tilde{S}_{ij}$, is written so that to be a sink of filtered kinetic energy when $\Pi_{sgs}^u > 0$ and a source when $\Pi_{sgs}^u < 0$ (i.e., backscatter). The value Π_{sgs}^u defines the amount of energy which transfers from large scale to subgrid scale and Π_{sgs}^u depends from SGS models that is used to find the subgrid tensor τ_{ij}^u.

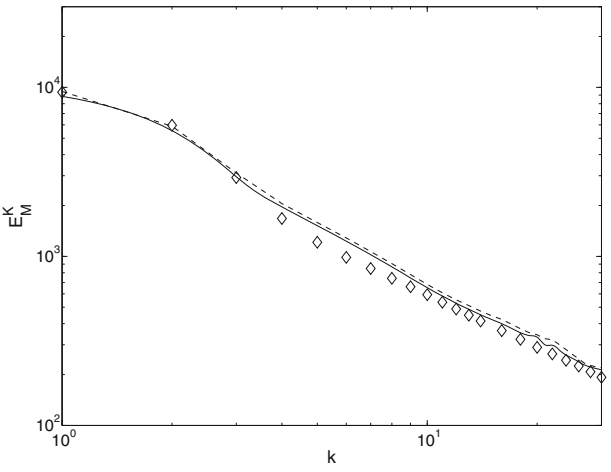

Fig. 10 Magnetic energy spectrum E_M^K for the first case. Symbols as in Fig. 5

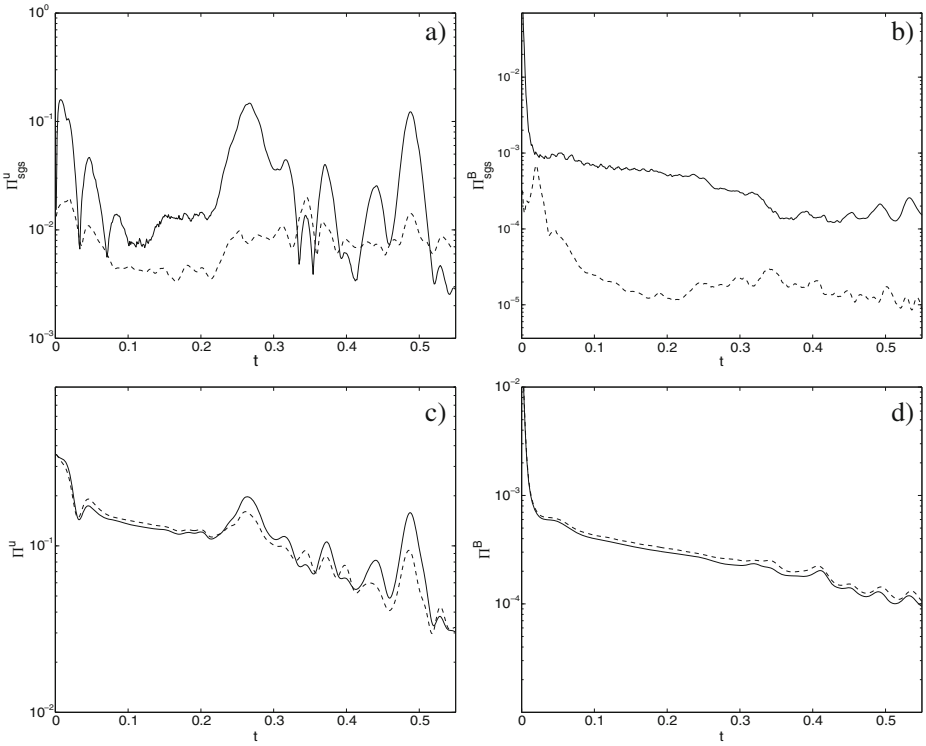

Fig. 11 Time dynamics of the kinetic energy subgrid scale dissipation $\prod_{sgs}^{u}$ (**a**), the magnetic energy subgrid scale dissipation $\prod_{sgs}^{B}$ (**b**), the molecular dissipation $\prod^{u}$ (**c**) and the magnetic molecular dissipation $\prod^{B}$ (**d**) for the first case. Symbols as in Fig. 5

The time dynamics of the molecular dissipation $\Pi^u = 2\mu \tilde{S}_{ij}\tilde{S}_{ij}$ is presented in Fig. 11c and Π^u is always positive. Note that linear forcing acts all the way down to the dissipative scale of turbulence. The magnetic energy subgrid scale dissipation in Fig. 11b is determined as $\Pi^B_{sgs} = -\tau^b_{ij}\bar{J}_{ij}$, and represents the large-scale energy drained by the subgrid scales, forward scatter corresponds to $\Pi^B_{sgs} > 0$ and backscatter to $\Pi^B_{sgs} < 0$. The magnetic molecular dissipation of turbulent field is defined as $\Pi^B = \eta|\bar{j}|^2$ and is shown in Fig. 11d. The magnetic energy subgrid scale dissipation is less for scale-similarity model while Smagorinsky closure is more dissipative model (see Fig. 11b). Therefore, scale-similarity model is more accurate SGS parametrization for time evolution of b_{rms} in Fig. 6 but Smagorinsky model turns out excessively dissipative one.

The second case of compressible MHD turbulence considered in the present paper corresponds the case when the similarity numbers are: $Re \approx 650$, $Re_M \approx 20$, $M_s \approx 0.23$, $M_a \approx 2.0$, $\gamma = 1.5$. The time evolution of root-mean-square velocity u_{rms} is shown in Fig. 12. In initial transient period, DNS results of u_{rms} drop very fast and then able to recover and to achieve a stationary average value. The transient period is longer for the second case than for the first case and the values of u_{rms} oscillate weaker. The both SGS models produce adequate results and show good agreement

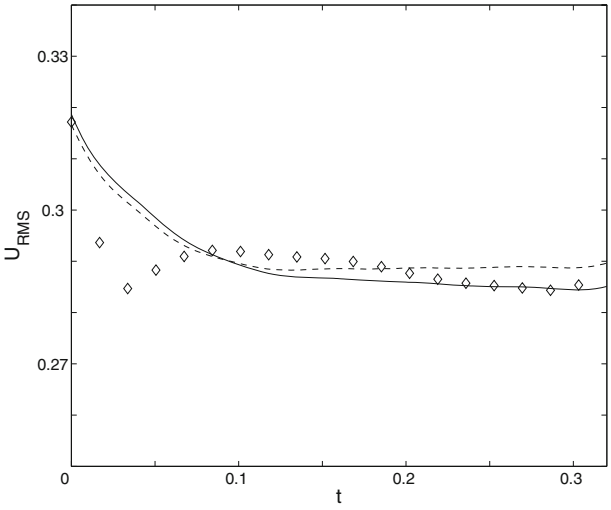

Fig. 12 Time evolution of u_{rms} for the second case. Symbols as in Fig. 5

with DNS results in stationary regime. From the time evolution of B_{rms} shown in Fig. 13, we can see that initially magnetic field increases rapidly and then attains statistically stationary level. The DNS results achieve this stationary level faster than SGS parameterizations. Referring to Fig. 13, the scale-similarity model provide more accurately results then the Smagorinsky model for compressible MHD turbulence. The Smagorinsly model is more dissipative SGS closure again. It should be indicated that these results coincide with the conclusion of the article [24] that Smagorinsky parametrization describes the flow well but not the magnetic field. Notice that the scale-similarity model for MHD is more precise one as well as in the first case. Time dynamics of the density is presented in Fig. 14 for the second case. Initially, there is large discrepancy in the results of the SGS models and the DNS results, but upon

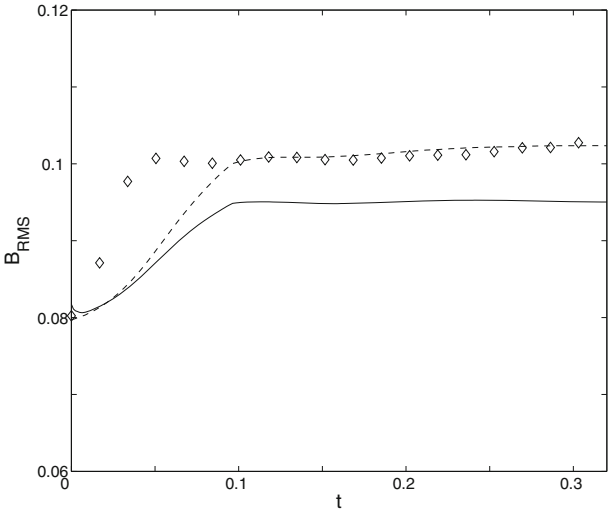

Fig. 13 Time evolution of B_{rms} for the second case. Symbols as in Fig. 5

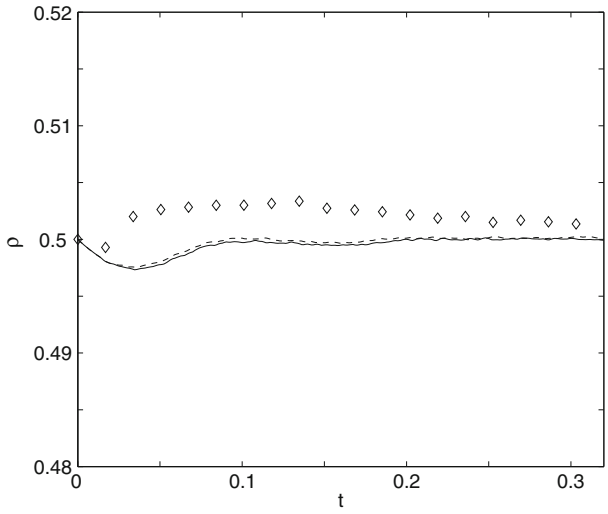

Fig. 14 Time dynamics of the density for the second case. Symbols as in Fig. 5

reaching steady state, these differences diminish. The spectrum of the total energy E_T^K is plotted in Fig. 15. The results of both SGS models are close to one another but scale-similarity model is slightly more accurate model as observed in Fig. 15.

The third case corresponds to the numerical computations when the similarity numbers are: $Re \approx 100$, $Re_M \approx 100$, $M_s \approx 0.52$, $M_a \approx 1.0$, $\gamma = 1.67$. Note that in considering this case, the Reynolds number and magnetic Reynolds number have the same value. The root-mean-square velocity u_{rms} as a function of time is shown in Fig. 16. As can be seen from Fig. 16, both SGS models reproduce well the velocity fluctuations with time. Differences between the results of DNS and subgrid-scale parameterizations are observed at the initial time interval when DNS results drop faster and then all the results are very close. Notice that the extended Smagorinsky

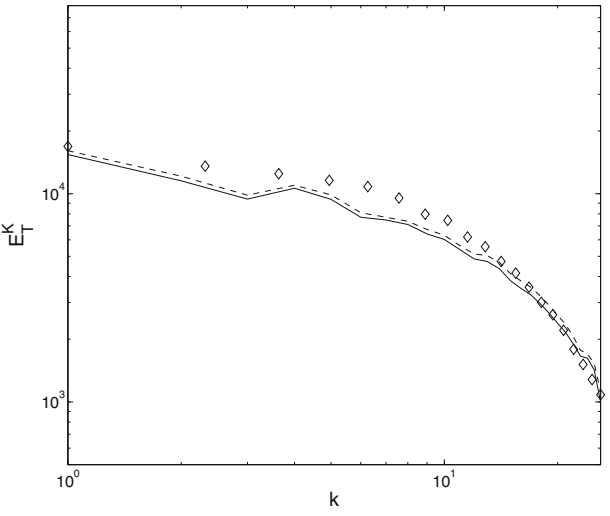

Fig. 15 Total energy spectrum E_T^K for the second case. Symbols as in Fig. 5

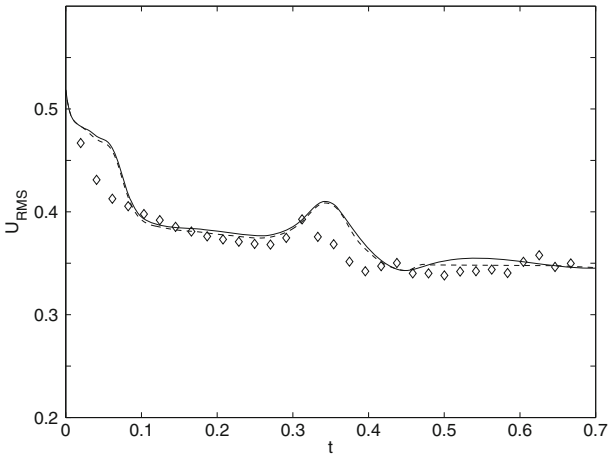

Fig. 16 Time evolution of u_{rms} for the third case. Symbols as in Fig. 5

model and the scale-similarity model for compressible MHD turbulence give almost identical results for u_{rms} in this case. Perhaps, this is related to not very high Reynolds number Re used in this run. Time dynamics of the root-mean-square magnetic field B_{rms} is presented in Fig. 17. In the transient period of time, the results of DNS decrease faster and then grow faster a little as compared with the results of the Smagorinsky model. The extended Smagorinsky parametrization is less accurate than the scale-similarity one for the the magnetic field. This conforms to conclusion that was discussed previously in the other numerical cases. As follows from Fig. 17 for the third case, the scale-similarity model provides accurate results and these results agree reasonably well with the DNS results of B_{rms} in the stationary regime of MHD turbulence. It must be noted that the rate of the attainment of a steady state depends on the initial distribution of the magnetic field and the velocity fluctuations and the initial similarity numbers.

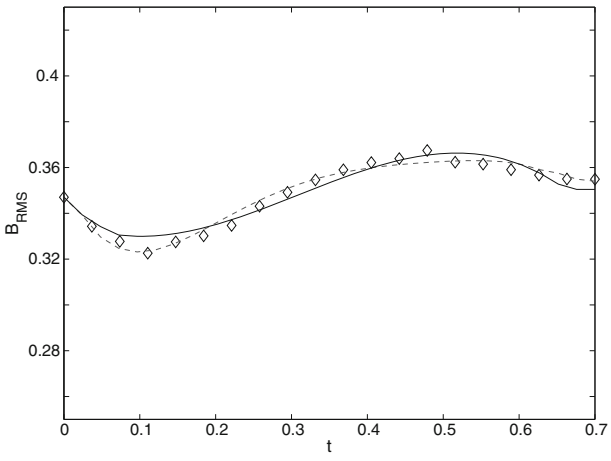

Fig. 17 Time evolution of B_{rms} for the third case. Symbols as in Fig. 5

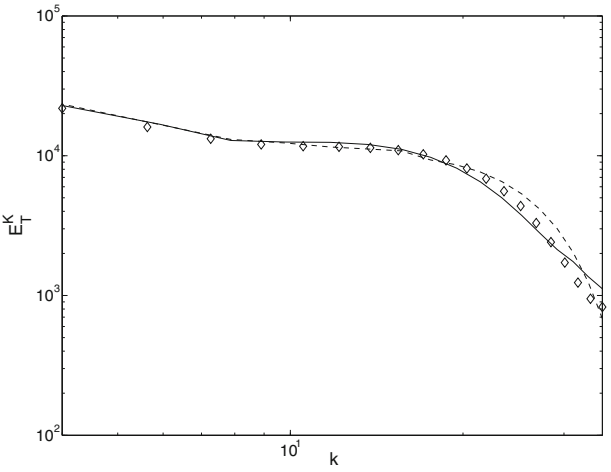

Fig. 18 Total energy spectrum E_T^K for the third case. Symbols as in Fig. 5

In Fig. 18, the total energy spectrum E_T^K is displayed. Differences in results are mainly observed at small scales. Both subgrid models give adequate results and it is difficult to identify which one is better for E_T^K. The magnetic energy spectrum E_M^K is shown in Fig. 19. As can be seen from Fig. 19, the DNS results are in good accordance with the scale-similarity model and the Smagorinsky one produces less accurate results. This is consistent with Fig. 17, which shows the time evolution of the magnetic field B_{rms}. As evident from Figs. 17 and 19, the scale-similarity model provides more accurate results for magnetic field compared with the Smagorinsky model for MHD case. It is clear that the scale-similarity model has excellent agreement with the results of DNS and can be used for modeling of compressible MHD turbulence and the scale-similarity closure can serve as a stand alone subgrid model.

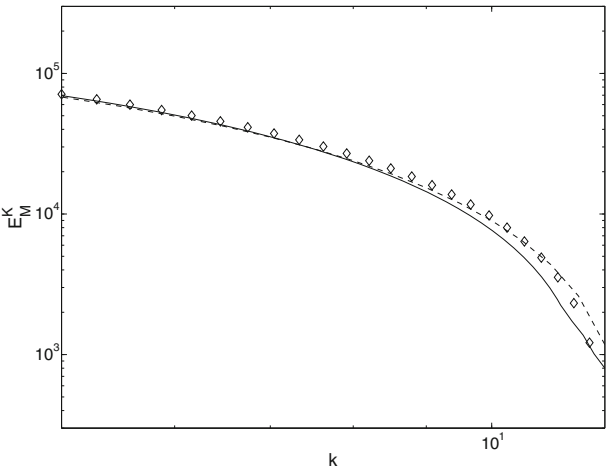

Fig. 19 Magnetic energy spectrum E_M^K for the third case. Symbols as in Fig. 5

4 Conclusions

The present study demonstrates that the scale-similarity model for forced MHD turbulence can be used as a stand alone SGS model as opposed to decaying case. The scale-similarity parametrization has evident advantages the main ones being to reproduce rightly the correlation between the tensors between actual and model turbulent stress tensor for isotropic flow as well as for anisotropic fluid flow, and the absence of special model constants in contrast to other SGS closures. However, the scale-similarity model does not dissipate energy enough and usually leads to inaccurate results in decaying turbulence or blows up the simulation. But the situation changes significantly when a forced turbulence is considered. In this case, subgrid modeling in LES approach have to provide correct stationary regime of the turbulence rather than to guarantee proper energy dissipation. Therefore, in the present work LES method for modeling of compressible forced MHD turbulence is applied for various similarity parameters. Driving forces in our calculations were determined by linear forcing theory. Numerical computations were carried out and the obtained results were analyzed by means of comparison with results of direct numerical simulation. It was shown that the scale-similarity model provides good accuracy and the results of this SGS model agree well with the DNS results. If differences between the results obtained by the scale-similarity model and the Smagorinsky closure for velocity field are insignificant, then the differences are considerable for magnetic field. For the magnetic field, discrepancies with the DNS results are substantially lower for scale-similarity model while the Smagorinsky parametrization for MHD is more dissipative and the results of Smagorinsky model are worse in agreement with DNS. The scale-similarity model is generally found to reproduce DNS results better.

Also, influence of discrete filter shapes on the scale-similarity model was examined. It was shown that the Gaussian filter is more sensitive to the parameter ϵ (the ratio of the mesh size to the cut-off lengthscale of the filter) than the top-hat one for scale-similarity model in compressible MHD turbulence. The 3-point filters give the worst results and the 5-point Gaussian filter demonstrates the best results at $\epsilon = 2$.

Thus, the scale-similarity model demonstrates more accurate results than the eddy-viscosity SGS model especially for the time evolution of the magnetic field. The obtained results show that the scale-similarity model might be a useful parametrization for simulating MHD turbulent system with driving forces and for study of scale-invariance properties of forced compressible MHD turbulence in the inertial range.

Acknowledgements Alexander Chernyshov gratefully acknowledges the financial support from Dynasty Foundation and Grant of President of Russian Federation for supporting young Russian scientists (MK-1349.2011.2). This work was partly supported by Russian Foundation for Basic Research (11-02-00805-a).

References

1. Agullo, O., Müller, W.C., Knaepen, B., Carati, D.: Large Eddy simulation of decaying magnetohydrodynamic turbulence with dynamic subgrid-modeling. Phys. Plasmas **8**(7), 3502–3505 (2001)

2. Balarac, G., Kosovichev, A.G., Brugiere, O., Wray, A., Mansour, N.: Modeling of the subgrid-scale term of the filtered magnetic field transport equation. In: Center for Turbulence Research Proceedings of the Summer Program 2010, pp. 503–512 (2010)
3. Bardina, J., Ferziger, J.H., Reynolds, W.C.: Improved subgrid scale models for Large Eddy simulation. In: AIAA 13th Fluid and Plasma Dynamics Conference, p. 10. Snowmass, Colo (1980)
4. Biskamp, D.: Magnetohydrodynamic Turbulence. Cambridge University Press, UK (2003)
5. Brandenburg, A.: The inverse cascade and nonlinear alpha-effect in simulations of isotropic helical hydromagnetic turbulence. Astrophys. J. **550**, 824–840 (2001). doi:10.1086/319783
6. Brandenburg, A.: Advances in theory and simulations of large-scale dynamos. Space Sci. Rev. **144**, 87–104 (2009). doi:10.1007/s11214-009-9490-0
7. Brandenburg, A.: Nonlinear small-scale dynamos at low magnetic prandtl numbers. Astrophys. J. **741**, 92 (2011). doi:10.1088/0004-637X/741/2/92
8. Brandenburg, A., Dobler, W.: Hydromagnetic turbulence in computer simulations. Comput. Phys. Commun. **147**, 471–475 (2002)
9. Brandenburg, A., Schmitt, D.: Simulations of an alpha-effect due to magnetic buoyancy. Astron. Astrophys. **338**, L55–L58 (1998)
10. Brandenburg, A., Subramanian, K.: Astrophysical magnetic fields and nonlinear dynamo theory. Phys. Rep. **417**, 1–209 (2005)
11. Chernyshov, A.A., Karelsky, K.V., Petrosyan, A.S.: Large-Eddy simulation of magnetohydrodynamic turbulence in compressible fluid. Phys. Plasmas **13**(3), 032,304 (2006)
12. Chernyshov, A.A., Karelsky, K.V., Petrosyan, A.S.: Subgrid-scale modelling of compressible magnetohydrodynamic turbulence in heat-conducting plasma. Phys. Plasmas **13**(10), 104,501 (2006)
13. Chernyshov, A.A., Karelsky, K.V., Petrosyan, A.S.: Development of Large Eddy simulation for modeling of decaying compressible mhd turbulence. Phys. Fluids **19**(5), 055,106 (2007)
14. Chernyshov, A.A., Karelsky, K.V., Petrosyan, A.S.: Assessment of subgrid-scale models for decaying compressible mhd turbulence. Flow Turbulence Combust. **80**(1), 21–35 (2008). doi:10.1007/s10494-007-9100-8
15. Chernyshov, A.A., Karelsky, K.V., Petrosyan, A.S.: Modeling of compressible magnetohydrodynamic turbulence in electrically and heat conducting fluid using Large Eddy simulation. Phys. Fluids **20**(8), 085,106 (2008)
16. Chernyshov, A.A., Karelsky, K.V., Petrosyan, A.S.: Validation of Large Eddy simulation method for study of flatness and skewness of decaying compressible magnetohydrodynamic turbulence. Theor. Comput. Fluid Dyn. **23**(6), 451–470 (2009)
17. Chernyshov, A.A., Karelsky, K.V., Petrosyan, A.S.: Forced turbulence in Large Eddy simulation of compressible magnetohydrodynamic turbulence. Phys. Plasmas **17**(10), 102,307 (2010)
18. Ferziger, J.: Large Eddy simulation. In: Gatski, T., Hussami, Y., Lumley, J. (eds.) Simulation and Modeling of Turbulent Flows, pp. 109–154. Oxford University Press, New York (1996)
19. Garnier, E., Adams, N., Sagaut, P.: Large Eddy Simulation for Compressible Flows. Springer Science+Business Media B.V., Netherlands (2009)
20. Germano, M., Piomelli, U., Moin, P., Cabot, W.: A dynamic subgrid-scale eddy-viscosity model. Phys. Fluids A **3**(7), 1760–1765 (1991)
21. Gomez, T., Sagaut, P., Schilling, O., Zhou, Y.: Large-Eddy simulation of very large kinetic and magnetic reynolds number isotropic magnetohydrodynamic turbulence using a spectral subgrid model. Phys. Fluids **19**(4), 032,304 (2007)
22. Grappin, R., Leorat, J., Pouquet, A.: Dependence of MHD turbulence spectra on the velocity field-magnetic field correlation. Astron. Astrophys. **126**, 51–58 (1983)
23. Hamba, F., Tsuchiya, M.: Cross-helicity dynamo effect in magnetohydrodynamic turbulent channel flow. Phys. Plasmas **17**(1), 012301-012301-13 (2010)
24. Haugen, N.E.L., Brandenburg, A.: Hydrodynamic and hydromagnetic energy spectra from Large Eddy simulations. Phys. Fluids **18**(7), 075,106 (2006). doi:10.1063/1.2222399
25. Knaepen, B., Moin, P.: Large-Eddy simulation of conductive flows at low magnetic reynolds number. Phys. Fluids **16**(5), 1255–1261 (2004)
26. Kolmogorov, A.N.: The local structure of turbulence in incomressible viscous fluids for very large reynolds numbers. Dokl. Akad. Nauk SSSR **30**(4), 19–21 (1941)
27. Leonard, A.: Energy cascade in Large Eddy simulations of turbulent fluid flows. Adv. Geophys. **18**, 237–248 (1974)
28. Leslie, D.C., Quarini, G.L.: The application of turbulence theory to the formulation of subgrid modelling procedures. J. Fluid Mech. **91**, 65–91 (1979). doi:10.1017/S0022112079000045

29. Liu, S., Meneveau, C., Katz, J.: On the properties of similarity subgridscale models as deduced from measurements in a turbulent jet. J. Fluid Mech. **275**, 83–119 (1994)
30. Low, M.M.M., Klessen, R.S., Burkert, A., Smith, M.D.: Kinetic energy decay rates of supersonic and super-alfvenic turbulence in star-forming clouds. Phys. Rev. Lett. **80**, 2754–2764 (1998)
31. Lundgren, T.S.: Linearly Forced Isotropic Turbulence. Center for Turbulence Research Annual Research Briefs, pp. 461–473 (2003)
32. Meneveau, C., Katz, J.: Scale-invariance and turbulence models for Large-Eddy simulation. Annu. Rev. Fluid Mech. **32**, 1–32 (2000)
33. Morinishi, Y., Vasilyev, O.V.: A recommended modification to the dynamic two-parameter mixed subgrid scale model for Large Eddy simulation of wall bounded turbulent flow. Phys. Fluids **13**, 3400–3410 (2001)
34. Müller, W.C., Carati, D.: Dynamic gradient-diffudion subgrid models for incompressible magnetohydrodynamics turbulence. Phys. Plasmas **9**(3), 824–834 (2002)
35. Piomelli, U., Ferziger, J.H., Moin, P.: Model consistency in Large Eddy simulation of turbulent channel flows. Phys. Fluids **31**, 1884–1891 (1988). doi:10.1063/1.866635
36. Pope, S.B.: Ten questions concerning the Large-Eddy simulation of turbulent flows. New J. Phys. **35**(1), 35 (2004)
37. Rosales, C., Meneveau, C.: Linear forcing in numerical simulations of isotropic turbulence: physical space implementations and convergence properties. Phys. Fluids **17**(9), 0951061-095106-8 (2005)
38. Sagaut, P.: Large Eddy Simulation for Incompressible Flows: An Introduction. Springer Verlag, Berlin Heidelberg (2002)
39. Sagaut, P., Comte, P., Ducros, F.: Filtered subgrid-scale models. Phys. Fluids **12**, 233–236 (2000). doi:10.1063/1.870297
40. Sagaut, P., Grohens, R.: Discrete filters for Large Eddy simulation. Int. J. Numer. Mech. Fluids **31**, 1195–1220 (1999)
41. Speziale, G.: Galilean invariance of subgrid-scale stress models in les of turbulence. J. Fluid Mech. **156**, 55–62 (1985)
42. Stefano, G.D., Vasilyev, O.V.: Stochastic coherent adaptive Large Eddy simulation of forced isotropic turbulence. J. Fluid Mech. **646**, 453–470 (2010)
43. Vorobev, A., Zikanov, O.: Smagorinsky constant in les modeling of anisotropic mhd turbulence. Theor. Comput. Fluid Dyn. **22**(3–4), 317–325 (2007)
44. Vreman, B., Geurts, B., Kuerten, H.: Subgrid-modeling in les of compressible flow. Appl. Sci. Res. **54**, 191–203 (1995)
45. Yokoi, N., Rubinstein, R., Yoshizawa, A., Hamba, F.: A turbulence model for magnetohydrodynamic plasmas. J. Turbul. **9**, 37 (2008). doi:10.1080/14685240802433057